# Molecular profiling reveals a hypoxia signature in breast implant-associated anaplastic large cell lymphoma

**Naoki Oishi,[1,2] Tanya Hundal,[1] Jessica L. Phillips,[1] Surendra Dasari,[1] Guangzhen Hu,[1] David S. Viswanatha,[1] Rong He,[1] Ming Mai,[1] Hailey K. Jacobs,[1] Nada H. Ahmed,[1,3] Sergei I. Syrbu,[4] Youssef Salama,[1] Jennifer R. Chapman,[5] Francisco Vega,[5°] Jagmohan Sidhu,[6] N. Nora Bennani,[7] Alan L. Epstein,[8] L. Jeffrey Medeiros,[9] Mark W. Clemens,[10#] Roberto N. Miranda[9#] and Andrew L. Feldman[1#]**

[1]Department of Laboratory Medicine and Pathology, Mayo Clinic, Rochester, MN, USA; [2]Department of Pathology, University of Yamanashi, Chuo, Yamanashi, Japan; [3]Department of Clinical Pathology, Suez Canal University, Ismailia, Egypt; [4]Department of Pathology, University of Iowa, Iowa City, IA, USA; [5]Department of Pathology, University of Miami, Miami, FL, USA; [6]Department of Pathology and Laboratory Medicine, United Health Services, Binghamton, NY, USA; [7]Division of Hematology, Mayo Clinic, Rochester, MN, USA; [8]Department of Pathology, University of Southern California Keck School of Medicine, Los Angeles, CA, USA; [9]Department of Hematopathology, MD Anderson Cancer Center, Houston, TX, USA and [10]Department of Plastic Surgery, MD Anderson Cancer Center, Houston, TX, USA

*°Current affiliation: Department of Hematopathology, MD Anderson Cancer Center, Houston, TX, USA*

*#MWC, RNM, and ALF contributed equally as co-senior authors.*

 doi:10.3324/haematol.2019.245860

Received: December 20, 2019.

Accepted: May 14, 2020.

Pre-published: May 15, 2020.

Correspondence: *ANDREW L. FELDMAN* - feldman.andrew@mayo.edu

# Molecular Profiling Reveals a Hypoxia Signature in Breast Implant-associated Anaplastic Large Cell Lymphoma

Oishi N et al.

## Supplemental Material

## Supplemental Methods

### Cell lines

Cell lines TLBR-1, TLBR-2, and TLBR-3 were established from BIA-ALCLs by A.L.E.[1, 2] and were maintained in RPMI-1640 (Gibco) supplemented with 10% FBS (Clontech), 1% penicillin/streptomycin (Gibco), and 100 U/mL IL2 (R&D 202-IL-050). TLBR-1, -2, and -3 cells were cultured at a concentration of 0.5 x $10^6$/mL for 72 h and resuspended in PBS. For experiments involving hypoxia, cells were incubated for 12-24 h at 37ºC under humidified conditions in a Napco Series 8000 water-jacketed $CO_2$ incubator (Thermo Scientific) at 5% $CO_2$ and 1% $O_2$. For siRNA electroporation, cells in the same media without addition of penicillin/streptomycin were transfected with siRNA targeting *CA9* (ON-TARGETplus SMARTpool, L-005244-00-0010; Dharmacon) or a non-targeting control pool (ON-TARGETplus, D-001810-10-05). Protein expression and cell proliferation were assessed after 72 h as described below.

### Western blotting

For western blotting, proteins were isolated from cell culture lysates in radioimmunoprecipitation assay (RIPA) buffer containing HALT, PMSF and Roche cOmplete™ Mini protease inhibitors.

Proteins were quantified using the Biorad DC™ assay and equal quantities were loaded and run on 10% Tris-HCl poly-acrylamide gels. Proteins were then transferred to nitrocellulose membranes and blocked with 1:1 TBS:Odyssey Blocking Buffer (LI-COR). Membranes were incubated overnight with the following primary antibodies: CA9 Rabbit mAb (D47G3; Cell Signaling), β-Actin (AC-15; Novus Biologicals LLC, Littleton, CO) and HIF-1α (EP1215Y; Abcam). Protein detection was performed on a LI-COR Odyssey Fc using IRDye® 680W and 800CW secondary antibodies (LI-COR).

**Cell proliferation assay**

The MTS assay (CellTiter 96® AQueous Non-Radioactive Cell Proliferation Assay, Promega) was used to assess cell viability per the manufacturer's protocol. Briefly, 50,000 cells were plated per well after electroporation with control or *CA9* siRNA. Plates were incubated under normoxic conditions for 48 h to allow cell recovery and then cultured under either normoxic or hypoxic conditions for 24 h. Colorimetric determination was performed measuring absorbance at 490 nm after incubation with MTS reagent for 2-3 h.

**Lentiviral CA9 overexpression**

Lentiviral vectors included a commercially available human CA9 lentiviral vector (pLenti-GIII-EF1a, ABM Inc., #LV102843) and empty pLenti-GIII-EF1a vector as a control (ABM Inc., #LV588). For viral packaging, 293T cells were maintained using DMEM complete media supplemented with 10% FBS. On the day of viral packaging, cell media was changed to RPMI1640 complete media supplemented with 10% FBS. Transfection solution was prepared in Opti-MEM™ I Reduced Serum Medium (Thermo Fisher Scientific, 31985070) using

Lipofectamine 3000 (Thermo Fisher Scientific, L3000015), lentiviral packaging plasmid psPAX2 (a gift from Didier Trono [Addgene plasmid #12260; http://n2t.net/addgene:12260; RRID:Addgene_12260]), and pMD2.G (a gift from Didier Trono [Addgene plasmid #12259; http://n2t.net/addgene:12259; RRID:Addgene_12259]), and added dropwise onto 293T cells. Packaged virus was harvested 24 h after transfection and purified by high speed centrifugation and filtration using 0.45 μm syringe filters (Fisher, 09-719D). TLBR-3 cells were maintained in RPMI1640 complete media supplemented with 10% FBS and IL2, transfected using titrated virus and polybrene (10 mg/mL), and selected in puromycin. Ten NSG mice per group were injected subcutaneously with 1.0 x $10^6$ cells TLBR-3 cells transduced with CA9 or empty vector in 100 μL of PBS and tumors were measured as described.

**Serum and tumor CA9 determination in BIA-ALCL xenograft models**

Eight NSG mice per group were injected subcutaneously with 10.0 x $10^6$ cells TLBR-1, -2, or -3 cells in 100 μL of PBS. When each tumor reached 1,000 $mm^3$ the corresponding mouse was euthanized and blood was obtained by cardiac puncture. Blood was similarly obtained from a fourth group of mice injected with PBS only. Blood samples were immediately stored in serum separator tubes (BD Microtainer), allowed to clot for 1 h, and centrifuged to collect serum. Subcutaneous tumors were harvested from tumor-bearing mice immediately after euthanasia. Tumor tissue was pulverized and lysed for 15 min on ice using RNase-free disposable pellet pestles (Fischer Scientific) in 120 μL of RIPA buffer containing HALT, PMSF, and Roche cOmplete™ Mini protease inhibitors. Samples were centrifuged at 13,000 rpm for 15 min at 4°C. Supernatant protein concentrations were determined using a DC protein assay and adjusted to a concentration of 1 μg/μL for CA9 measurement by ELISA.

**CA9 ELISA**

Human serum (n=1), plasma (n=3), and seroma (n=13) samples were collected at MD Anderson Cancer Center between May 2014 and March 2019 as previously published.[3] Ten seromas were involved by BIA-ALCL based on standard pathologic criteria.[4] Control seromas were collected from 3 patients, 2 with benign seromas and 1 from an uninvolved seroma contralateral to BIA-ALCL. CA9 concentrations in seroma, serum, plasma, cell culture supernatant, and tumor lysate samples were measured using a commercially available solid-phase ELISA kit (Quantikine, R&D Systems, Minneapolis, MN) following the manufacturer's instructions, diluting samples as needed to allow interpretation within the dynamic range of the reference standard curve. Briefly, 100 µL of appropriately diluted sample was added to each well and the plate was shaken for 2 h at room temperature. Wells were washed, incubated with 200 µL of biotinylated anti-CA9 conjugate for 2 h, washed again, and then incubated with 200 µL of streptavidin-horseradish peroxidase and stabilized chromogen solution for 0.5 h. Finally, 50 µL of stop solution (2N $H_2SO_4$) was added and absorbance was measured at 450 nm on a photometric plate reader. Concentrations were interpolated from triplicate measurements using a second-order polynomial quadratic model.

**Statistical analysis**

Statistical analyses were performed using JMP Pro 14 (SAS Institute), GraphPad Prism 7, or in the R statistical environment. Statistical tests are as indicated. P-values $<0.05$ were considered statistically significant.

# Supplemental Tables

## Supplemental Table 1. Top gene sets positively associated with BIA-ALCLs

| NAME | NES | Nom P-val | FDR q-val |
|---|---|---|---|
| HALLMARK_EPITHELIAL_MESENCHYMAL_TRANSITION | 2.963 | 0.000 | 0.000 |
| HALLMARK_HYPOXIA | 2.727 | 0.000 | 0.000 |
| HALLMARK_TNFA_SIGNALING_VIA_NFKB | 2.530 | 0.000 | 0.000 |
| REACTOME_COLLAGEN_FORMATION | 2.358 | 0.000 | 0.000 |
| KEGG_ECM_RECEPTOR_INTERACTION | 2.140 | 0.000 | 0.001 |
| REACTOME_EXTRACELLULAR_MATRIX_ORGANIZATION | 2.139 | 0.000 | 0.001 |
| REACTOME_A_TETRASACCHARIDE_LINKER_SEQUENCE_IS_REQUIRED_FOR_GAG_SYNTHESIS | 2.072 | 0.000 | 0.002 |
| BIOCARTA_CDMAC_PATHWAY | 2.052 | 0.000 | 0.002 |
| HALLMARK_ANGIOGENESIS | 2.022 | 0.000 | 0.004 |
| REACTOME_ACTIVATION_OF_THE_AP1_FAMILY_OF_TRANSCRIPTION_FACTORS | 1.959 | 0.000 | 0.010 |

**Supplemental Table 2. Top gene sets associated with hypoxia vs. normoxia in TLBR-2 cells**

| NAME | NES | Nom P-val | FDR q-val |
|---|---|---|---|
| **Up-regulated Gene Sets** | | | |
| HALLMARK_HYPOXIA | 2.514 | 0.000 | 0.000 |
| HALLMARK_GLYCOLYSIS | 2.145 | 0.000 | 0.000 |
| REACTOME_3_UTR_MEDIATED_TRANSLATIONAL_REGULATION | 2.090 | 0.000 | 0.000 |
| REACTOME_NONSENSE_MEDIATED_DECAY_ENHANCED_BY_THE_EXON_JUNCTION_COMPLEX | 2.023 | 0.000 | 0.000 |
| KEGG_NITROGEN_METABOLISM | 1.950 | 0.000 | 0.002 |
| REACTOME_METABOLISM_OF_CARBOHYDRATES | 1.918 | 0.000 | 0.005 |
| REACTOME_GLUCOSE_METABOLISM | 1.920 | 0.000 | 0.005 |
| REACTOME_SRP_DEPENDENT_COTRANSLATIONAL_PROTEIN_TARGETING_TO_MEMBRANE | 1.894 | 0.000 | 0.010 |
| HALLMARK_IL2_STAT5_SIGNALING | 1.870 | 0.000 | 0.016 |
| HALLMARK_KRAS_SIGNALING_UP | 1.856 | 0.000 | 0.019 |
| KEGG_JAK_STAT_SIGNALING_PATHWAY | 1.846 | 0.000 | 0.022 |
| KEGG_CYTOKINE_CYTOKINE_RECEPTOR_INTERACTION | 1.842 | 0.000 | 0.022 |

| | | | |
|---|---|---|---|
| REACTOME_GLYCOLYSIS | 1.823 | 0.002 | 0.029 |
| KEGG_PENTOSE_PHOSPHATE_PATHWAY | 1.819 | 0.002 | 0.030 |
| REACTOME_GLUCONEOGENESIS | 1.823 | 0.000 | 0.031 |
| KEGG_STARCH_AND_SUCROSE_METABOLISM | 1.799 | 0.002 | 0.042 |
| **Down-regulated Gene Sets** | | | |
| HALLMARK_MYC_TARGETS_V2 | -1.937 | 0.000 | 0.001 |

**Supplemental Table 3. Top gene sets associated with *CA9* siRNA vs. control siRNA in TLBR-2 cells**

| NAME | NES | Nom P-val | FDR q-val |
|---|---|---|---|
| **Up-regulated Gene Sets** | | | |
| None passing FDR≤0.05 | | | |
| **Down-regulated Gene Sets** | | | |
| HALLMARK_MYC_TARGETS_V1 | -2.460 | 0.000 | 0.000 |
| REACTOME_S_PHASE | -2.236 | 0.000 | 0.000 |
| HALLMARK_MYC_TARGETS_V2 | -2.228 | 0.000 | 0.000 |
| REACTOME_ASSEMBLY_OF_THE_PRE_REPLICATIVE_COMPLEX | -2.143 | 0.000 | 0.000 |
| REACTOME_ORC1_REMOVAL_FROM_CHROMATIN | -2.174 | 0.000 | 0.000 |
| REACTOME_DNA_REPLICATION | -2.182 | 0.000 | 0.000 |
| HALLMARK_UNFOLDED_PROTEIN_RESPONSE | -2.191 | 0.000 | 0.000 |
| REACTOME_M_G1_TRANSITION | -2.135 | 0.000 | 0.000 |
| REACTOME_SYNTHESIS_OF_DNA | -2.198 | 0.000 | 0.000 |
| REACTOME_G1_S_TRANSITION | -2.129 | 0.000 | 0.000 |

| | | | |
|---|---|---|---|
| REACTOME_MITOTIC_M_M_G1_PHASES | -2.126 | 0.000 | 0.000 |
| REACTOME_HOST_INTERACTIONS_OF_HIV_FACTORS | -2.098 | 0.000 | 0.001 |
| REACTOME_REGULATION_OF_MITOTIC_CELL_CYCLE | -2.105 | 0.000 | 0.001 |
| KEGG_PROTEASOME | -2.095 | 0.000 | 0.001 |
| HALLMARK_E2F_TARGETS | -2.071 | 0.000 | 0.001 |
| REACTOME_VIF_MEDIATED_DEGRADATION_OF_APOBEC3G | -2.069 | 0.000 | 0.001 |
| REACTOME_REGULATION_OF_ORNITHINE_DECARBOXYLASE_ODC | -2.062 | 0.000 | 0.001 |
| REACTOME_MRNA_PROCESSING | -2.072 | 0.000 | 0.001 |
| REACTOME_MITOTIC_G1_G1_S_PHASES | -2.062 | 0.000 | 0.001 |
| REACTOME_SCF_BETA_TRCP_MEDIATED_DEGRADATION_OF_EMI1 | -2.063 | 0.000 | 0.001 |
| REACTOME_CDT1_ASSOCIATION_WITH_THE_CDC6_ORC_ORIGIN_COMPLEX | -2.063 | 0.000 | 0.001 |
| REACTOME_PROCESSING_OF_CAPPED_INTRON_CONTAINING_PRE_MRNA | -2.074 | 0.000 | 0.001 |
| REACTOME_CYCLIN_E_ASSOCIATED_EVENTS_DURING_G1_S_TRANSITION_ | -2.075 | 0.000 | 0.001 |
| REACTOME_APC_C_CDH1_MEDIATED_DEGRADATION_OF_CDC20_AND_OTHER_APC_C_CDH1_TARGETED_PROTEINS_IN_LATE_MITOSIS_EARLY_G1 | -2.075 | 0.000 | 0.001 |
| HALLMARK_MTORC1_SIGNALING | -2.075 | 0.000 | 0.001 |
| REACTOME_SCFSKP2_MEDIATED_DEGRADATION_OF_P27_P21 | -2.054 | 0.000 | 0.001 |
| REACTOME_CROSS_PRESENTATION_OF_SOLUBLE_EXOGENOUS_ANTIGENS_ENDOSOMES | -2.052 | 0.000 | 0.001 |

| | | | |
|---|---|---|---|
| REACTOME_APC_C_CDC20_MEDIATED_DEGRADATION_OF_MITOTIC_PROTEINS | -2.077 | 0.000 | 0.001 |
| REACTOME_ER_PHAGOSOME_PATHWAY | -2.079 | 0.000 | 0.001 |
| KEGG_ASTHMA | -2.045 | 0.000 | 0.001 |
| HALLMARK_INFLAMMATORY_RESPONSE | -2.035 | 0.000 | 0.002 |
| REACTOME_METABOLISM_OF_RNA | -2.037 | 0.000 | 0.002 |
| REACTOME_ACTIVATION_OF_NF_KAPPAB_IN_B_CELLS | -2.029 | 0.000 | 0.002 |
| REACTOME_CDK_MEDIATED_PHOSPHORYLATION_AND_REMOVAL_OF_CDC6 | -2.039 | 0.000 | 0.002 |
| REACTOME_DESTABILIZATION_OF_MRNA_BY_AUF1_HNRNP_D0 | -2.030 | 0.000 | 0.002 |
| REACTOME_AUTODEGRADATION_OF_CDH1_BY_CDH1_APC_C | -2.041 | 0.000 | 0.002 |
| REACTOME_TRNA_AMINOACYLATION | -2.003 | 0.000 | 0.002 |
| REACTOME_CELL_CYCLE_CHECKPOINTS | -2.000 | 0.000 | 0.002 |
| REACTOME_MRNA_SPLICING | -2.001 | 0.000 | 0.002 |
| REACTOME_CELL_CYCLE_MITOTIC | -1.978 | 0.000 | 0.004 |
| REACTOME_REGULATION_OF_APOPTOSIS | -1.970 | 0.000 | 0.005 |
| BIOCARTA_CD40_PATHWAY | -1.972 | 0.000 | 0.005 |
| REACTOME_MITOCHONDRIAL_PROTEIN_IMPORT | -1.941 | 0.000 | 0.009 |
| REACTOME_SIGNALING_BY_WNT | -1.941 | 0.000 | 0.009 |
| KEGG_SPLICEOSOME | -1.941 | 0.000 | 0.009 |

| | | | |
|---|---|---|---|
| REACTOME_REGULATION_OF_MRNA_STABILITY_BY_PROTEINS_THAT_BIND_AU_RICH_ELEMENTS | -1.942 | 0.002 | 0.009 |
| BIOCARTA_PROTEASOME_PATHWAY | -1.937 | 0.002 | 0.009 |
| HALLMARK_G2M_CHECKPOINT | -1.935 | 0.000 | 0.009 |
| REACTOME_ANTIGEN_PROCESSING_CROSS_PRESENTATION | -1.931 | 0.000 | 0.010 |
| HALLMARK_CHOLESTEROL_HOMEOSTASIS | -1.917 | 0.002 | 0.012 |
| REACTOME_PROTEIN_FOLDING | -1.914 | 0.000 | 0.012 |
| REACTOME_PREFOLDIN_MEDIATED_TRANSFER_OF_SUBSTRATE_TO_CCT_TRIC | -1.909 | 0.002 | 0.013 |
| REACTOME_CYTOSOLIC_TRNA_AMINOACYLATION | -1.905 | 0.004 | 0.013 |
| HALLMARK_UV_RESPONSE_UP | -1.902 | 0.000 | 0.014 |
| REACTOME_P53_DEPENDENT_G1_DNA_DAMAGE_RESPONSE | -1.896 | 0.002 | 0.015 |
| REACTOME_METABOLISM_OF_MRNA | -1.897 | 0.000 | 0.015 |
| KEGG_AMINOACYL_TRNA_BIOSYNTHESIS | -1.891 | 0.002 | 0.016 |
| REACTOME_P53_INDEPENDENT_G1_S_DNA_DAMAGE_CHECKPOINT | -1.887 | 0.004 | 0.016 |
| REACTOME_HIV_LIFE_CYCLE | -1.881 | 0.002 | 0.017 |
| REACTOME_LATE_PHASE_OF_HIV_LIFE_CYCLE | -1.874 | 0.000 | 0.018 |
| REACTOME_DOWNSTREAM_SIGNALING_EVENTS_OF_B_CELL_RECEPTOR_BCR | -1.876 | 0.000 | 0.018 |
| REACTOME_TRANSPORT_OF_MATURE_TRANSCRIPT_TO_CYTOPLASM | -1.875 | 0.004 | 0.018 |

| | | | |
|---|---|---|---|
| HALLMARK_ALLOGRAFT_REJECTION | -1.876 | 0.000 | 0.018 |
| REACTOME_CHOLESTEROL_BIOSYNTHESIS | -1.866 | 0.006 | 0.020 |
| REACTOME_METABOLISM_OF_NON_CODING_RNA | -1.862 | 0.002 | 0.020 |
| REACTOME_AUTODEGRADATION_OF_THE_E3_UBIQUITIN_LIGASE_COP1 | -1.864 | 0.002 | 0.020 |
| KEGG_ALLOGRAFT_REJECTION | -1.858 | 0.010 | 0.021 |
| BIOCARTA_TNFR2_PATHWAY | -1.851 | 0.000 | 0.022 |
| REACTOME_MRNA_SPLICING_MINOR_PATHWAY | -1.848 | 0.004 | 0.023 |
| REACTOME_INTERACTIONS_OF_VPR_WITH_HOST_CELLULAR_PROTEINS | -1.844 | 0.002 | 0.024 |
| KEGG_CYTOSOLIC_DNA_SENSING_PATHWAY | -1.838 | 0.013 | 0.025 |
| REACTOME_PERK_REGULATED_GENE_EXPRESSION | -1.836 | 0.004 | 0.025 |
| KEGG_JAK_STAT_SIGNALING_PATHWAY | -1.817 | 0.002 | 0.030 |
| KEGG_PYRIMIDINE_METABOLISM | -1.815 | 0.002 | 0.031 |
| REACTOME_TRANSCRIPTION | -1.807 | 0.000 | 0.031 |
| KEGG_DNA_REPLICATION | -1.808 | 0.008 | 0.031 |
| REACTOME_RNA_POL_II_TRANSCRIPTION | -1.808 | 0.000 | 0.032 |
| REACTOME_FORMATION_OF_TUBULIN_FOLDING_INTERMEDIATES_BY_CCT_TRIC | -1.809 | 0.008 | 0.032 |
| REACTOME_EXTENSION_OF_TELOMERES | -1.800 | 0.012 | 0.032 |
| HALLMARK_TNFA_SIGNALING_VIA_NFKB | -1.801 | 0.000 | 0.032 |

| | | | |
|---|---|---|---|
| BIOCARTA_RANMS_PATHWAY | -1.795 | 0.000 | 0.033 |
| REACTOME_DNA_STRAND_ELONGATION | -1.795 | 0.010 | 0.033 |
| REACTOME_CLEAVAGE_OF_GROWING_TRANSCRIPT_IN_THE_TERMINATION_REGION_ | -1.788 | 0.014 | 0.035 |
| KEGG_VIRAL_MYOCARDITIS | -1.779 | 0.006 | 0.037 |
| REACTOME_APOPTOSIS | -1.775 | 0.002 | 0.038 |
| BIOCARTA_RACCYCD_PATHWAY | -1.776 | 0.004 | 0.038 |
| REACTOME_INFLUENZA_LIFE_CYCLE | -1.769 | 0.000 | 0.039 |
| BIOCARTA_TH1TH2_PATHWAY | -1.759 | 0.006 | 0.042 |
| KEGG_AUTOIMMUNE_THYROID_DISEASE | -1.760 | 0.015 | 0.042 |
| BIOCARTA_41BB_PATHWAY | -1.760 | 0.000 | 0.042 |
| REACTOME_ACTIVATION_OF_THE_PRE_REPLICATIVE_COMPLEX | -1.747 | 0.016 | 0.045 |
| KEGG_STEROID_BIOSYNTHESIS | -1.747 | 0.013 | 0.045 |
| REACTOME_METABOLISM_OF_AMINO_ACIDS_AND_DERIVATIVES | -1.739 | 0.002 | 0.048 |

## Supplemental Figures

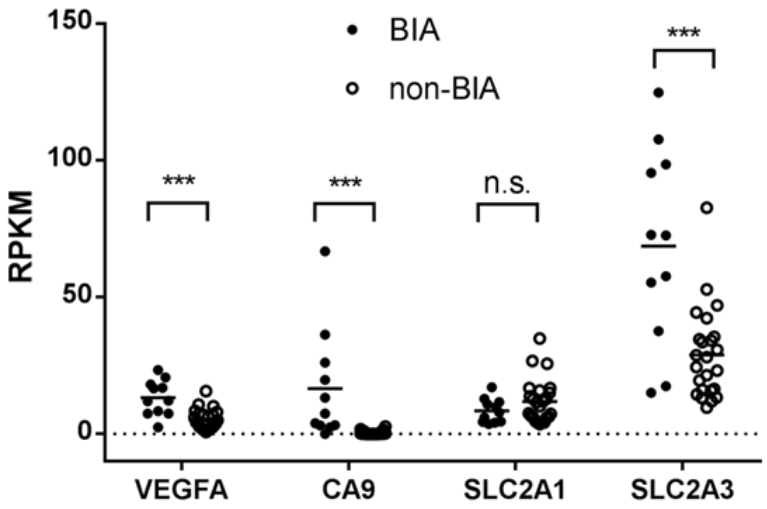


**Supplemental Figure 1.** BIA-ALCLs show significantly higher expression of hypoxia-related genes such as *VEGFA*, *CA9*, and *SLC2A3* encoding GLUT3 than non-BIA-ALCLs. No differential expression of *SLC2A1* encoding GLUT1 is observed. See also Figure 1, main manuscript. ***P<0.001; n.s., not significant.

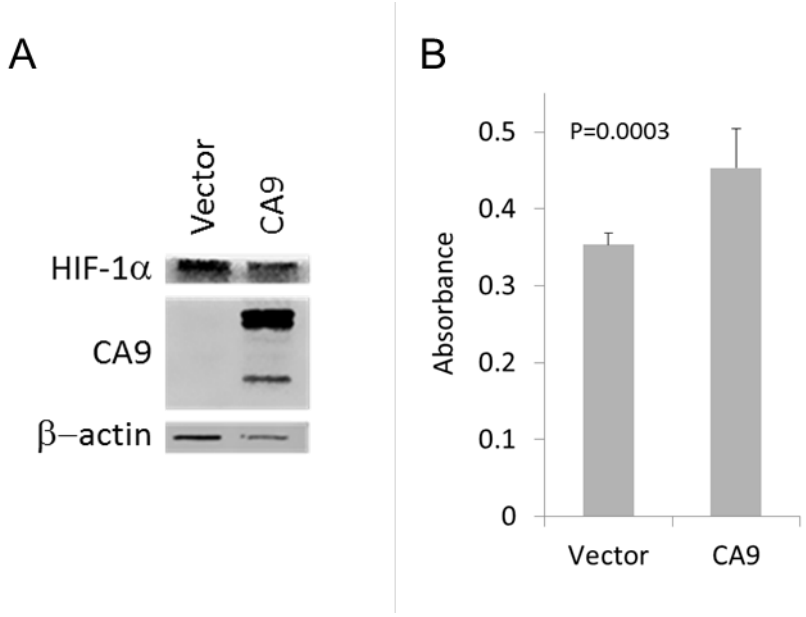


**Supplemental Figure 2. Effect of CA9 overexpression in vitro.** (A) Western blot showing CA9 expression in TLBR-3 cells stably transduced with CA9 lentivirus or control vector under hypoxic conditions. (B) Relative growth of TLBR-3 cells stably transduced with CA9 lentivirus or control vector (MTS assay).

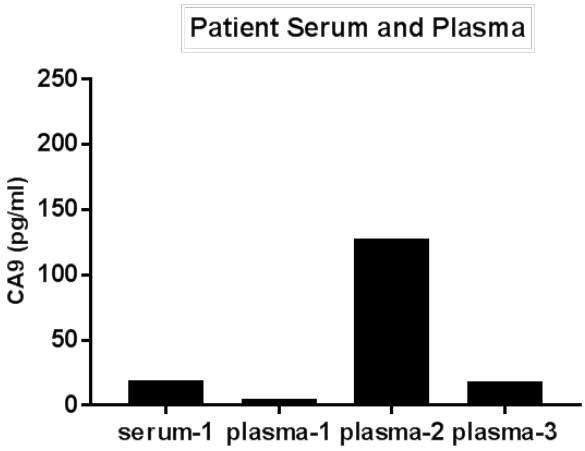


**Supplemental Figure 3.** Serum and plasma measurements of CA9 concentration in a limited number of samples from patients with BIA-ALCL.

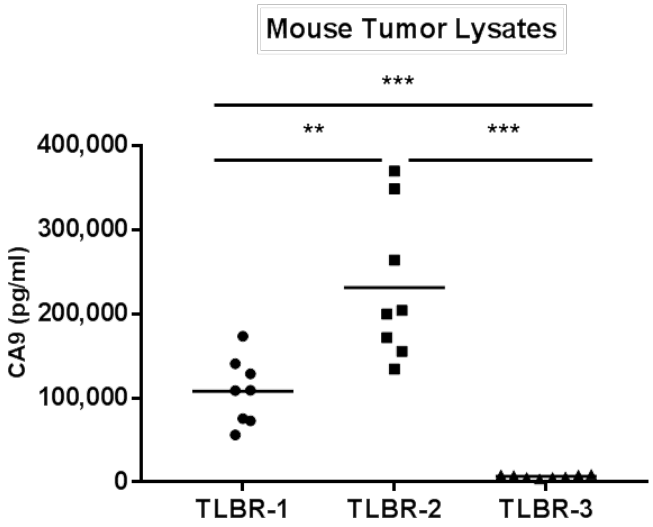


**Supplemental Figure 4.** Subcutaneous TLBR-1, -2, and -3 tumors were grown in NSG mice to a tumor volume of 1000 $mm^3$. Animals were euthanized and tumor tissue CA9 concentrations were measured by ELISA. See also Figure 6C. **, P<0.01; ***, P<0.001 (Mann-Whitney test).

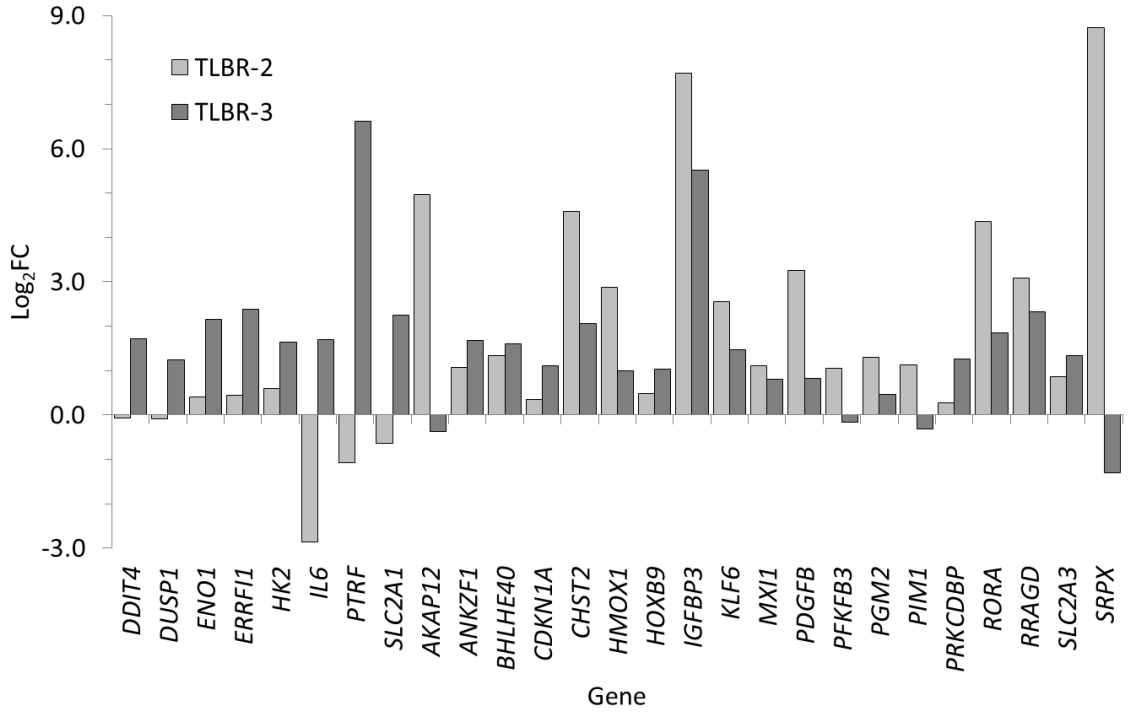


**Supplemental Figure 5.** Gene expression data were derived from RNA sequencing of TLBR-1, -2, and -3 cell lines at normoxic baseline. Genes from the HALLMARK HYPOXIA gene set with $\log_2$ fold-change (FC) values ≥1 in either TLBR-2 or TLBR-3 compared to TLBR-1 are shown.

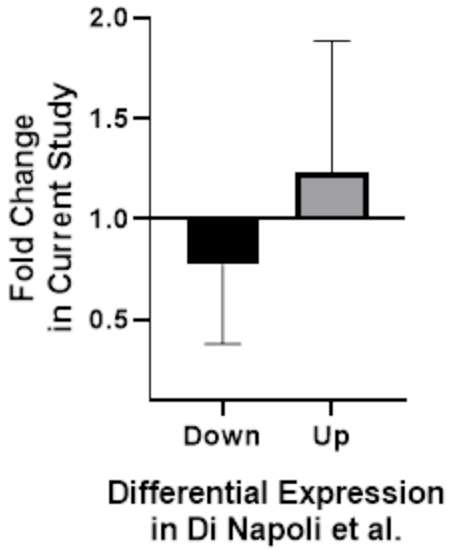


**Supplemental Figure 6.** Genes reported as significantly down- or up-regulated comparing BIA-ALCL to systemic ALCL in Di Napoli et al[5] were evaluated for fold-change differences in expression in the present study comparing BIA-ALCL to ALCLs of triple-negative genetic subtype. Means and standard deviations are shown.

## Supplemental References

1. Lechner MG, Lade S, Liebertz DJ, et al. Breast implant-associated, ALK-negative, T-cell, anaplastic, large-cell lymphoma: establishment and characterization of a model cell line (TLBR-1) for this newly emerging clinical entity. Cancer. 2011;117(7):1478-1489.

2. Lechner MG, Megiel C, Church CH, et al. Survival signals and targets for therapy in breast implant-associated ALK--anaplastic large cell lymphoma. Clin Cancer Res. 2012;18(17):4549-4559.

3. Hanson SE, Hassid VJ, Branch-Brooks C, et al. Validation of a CD30 Enzyme-Linked Immunosorbant Assay for the Rapid Detection of Breast Implant-Associated Anaplastic Large Cell Lymphoma. Aesthet Surg J. 2019;Feb 21. pii: sjy327. doi: 10.1093/asj/sjy327. [Epub ahead of print](

4. Feldman AL, Harris NL, Stein H, et al. Breast implant-associated anaplastic large cell lymphoma. In: Swerdlow SH, Campo E, Harris NL, Jaffe ES, Pileri SA, Stein H, et al., eds. WHO Classification of Tumours of Haematopoietic and Lymphoid Tissues. Revised 4th ed. Lyon: International Agency for Research on Cancer, 2017:421-422.

5. Di Napoli A, De Cecco L, Piccaluga PP, et al. Transcriptional analysis distinguishes breast implant-associated anaplastic large cell lymphoma from other peripheral T-cell lymphomas. Mod Pathol. 2019;32(2):216-230.